Modeling of NO x Formation and Consumption during Oxidation of Small Alcohols

Krishna Prasad Shrestha, Lars Seidel, Thomas Zeuch, Fabian Mauss

Modeling of NO_x Formation and Consumption during Oxidation of Small Alcohols

Krishna Prasad Shrestha*[1], Lars Seidel[2], Thomas Zeuch[3], and Fabian Mauss[1]

1. Thermodynamics and Thermal Process Engineering, Brandenburg University of Technology, Cottbus, Germany
2. LOGE Deutschland GmbH, Cottbus, Germany
3. Institut für Physikalische Chemie, Georg-August-Universität Göttingen, Göttingen, Germany

Abstract

This work presents a newly developed kinetic mechanism extending our recent work (Shrestha et al. [1]) for the oxidation of methanol and ethanol and their fuel interaction with NO_x chemistry in jet-stirred reactors, flow reactors, and burner-stabilized premixed flames. The work mainly focuses on fuel interaction with nitrogen chemistry and NO formation in laminar premixed flames. It is found that for methanol oxidation in jet-stirred reactor doping of the fuel blends with NO increase the reactivity of the system by increasing the net production of OH radicals. The increased amount of OH is formed *via* NO/NO_2 interconversion reaction channels $NO+HO_2 \leftrightharpoons NO_2+OH$, $NO_2+H \leftrightharpoons NO+OH$, $NO_2+HO_2 \leftrightharpoons HONO+O_2$, followed by the thermal decomposition of HONO producing NO and OH. In burner-stabilized premixed flames studied here for methanol/air and ethanol/air, NO is mainly formed *via* the NCN route ($CH+N_2 \leftrightharpoons NCN+H$) and minor contribution comes from the NNH route ($NNN \leftrightharpoons N_2+H$).

Introduction

Due to the increasing fuel consumption, fast depletion of fossil fuel resources is unavoidable. The stringent legislation of emission have boosted the advancement of alternative fuels for internal combustion engines applications. In the last decades, methanol/ethanol-gasoline blends have been investigated extensively and regarded as a potential alternative fuel for gasoline engines [2]. Combustion of fossil fuels emits hazardous pollutant gases, such as NO_x, carbon dioxide and sulfur oxides, which contribute significantly to the greenhouse effect. Hence, the search for environmentally friendly alternative or renewable fuel for use in internal combustion (IC) engines is taking the center stage globally. Among a wide range of available alcohols, primary alcohols such as methanol, ethanol, and butanol have the high potential for their utilization in the transportation sector, because they are cheaper than other alcohols and have physical and combustion related properties similar to gasoline and Diesel. Therefore, primary alcohols can be used in engines which employ conventional fueling technologies [3,4]. The higher octane rating of alcohols and the presence of oxygen in their molecular structure lead to their higher combustion efficiency and lower emission potential [5,6]. Alcohols have a higher latent heat of vaporization, therefore the alcohol–air mixture formed in the intake manifold is relatively cooler compared to a gasoline-air mixture. This produces relatively lower oxides of nitrogen (NO_x) emissions from an alcohol-fueled engine, as compared to gasoline, fueled engine [7]. There are number of studies in literature for the hydrocarbon/NO_x [8,9] interaction. However, there is a limited number of studies on alcohol/NO_x interaction from both experimental and numerical side.

To our best knowledge, there is no generally applicable kinetic model for alcohol combustion covering NO_x chemistry, which is validated over a broad range of experimental conditions. This situation calls for an in-depth analysis of NO_x interaction with the methanol and ethanol oxidation chemistry. The aim of the present work is to extend our recently published baseline mechanism Shrestha et al. [1] ($H_2/NH_3/CO/CH_4/NO_x$ kinetic model) to include methanol and ethanol as fuel and subsequently study their interaction with nitrogen chemistry by considering the available experiments from published literature in the validation process. This work is an ongoing effort to develop a comprehensive mechanism for fuel/NO_x interaction. The Model derived in this work is critically tested for speciation in plug flow reactors (PFR), in jet stirred reactors (JSR), and other burner stabilized flames (BSF), as well as for laminar flame speeds (LFS) and for ignition delay times (IDT).

Kinetic Model

The mechanism proposed here is the extension of our recently published work Shrestha et al. [1] which has been developed for $NH_3/H_2/CO/CH_4$ oxidation and NO_x chemistry interaction. The here derived $C_1 - C_2/NO_x$ model is based on published literature, as described in our previous work [1] wherever possible the rate parameters of the elementary reactions used in present work is adopted from Baulch et al. [10]. The NO_x sub-mechanism is augmented to include cross-reactions between nitrogen and carbon chemistry. The main objective is to include C_1/C_2 hydrocarbon species as fuel molecules. However, the focus of this study will be primarily on methanol (CH_3OH), ethanol (C_2H_5OH), and related NO_x kinetics.

Results and Discussion

Figure 1 shows the oxidation of CH_3OH in JSR in presence of 50 ppm of NO at $\phi = 1.0$, P = 1 atm, residence

*Corresponding author: shrestha@b-tu.de

time (τ) = 0.2 s studied by [11]. It is interesting to observe at different temperatures how NO/NO_2 interconversion takes place. The underlying chemistry for this NO/NO_2 interconversion process will be briefly discussed below. We can observe in Figure 1 at 720 K where unset of methanol oxidation is not yet begun but the conversion of NO to NO_2 is already started, which is mainly due to the reaction $NO+HO_2 \leftrightharpoons NO_2+OH$. At 860 K CH_3OH begins oxidizing with OH, H and HO_2 radicals forming CH_2OH as the major product and CH_3O as a minor product. At this temperature (860 K) NO is consumed rapidly and as expected NO_2 concentration peaks. The additional species that participates in the NO/NO_2 interconversion process at this temperature (860 K) is HONO. The main reaction that converts NO to NO_2 is $NO+HO_2 \leftrightharpoons NO_2+OH$, the formed NO_2 further reacts with CH_3OH and HO_2 to form HONO *via* reactions $CH_3OH+NO_2 \leftrightharpoons HONO+CH_2OH$ and $NO_2+HO_2 \leftrightharpoons HONO+O_2$.

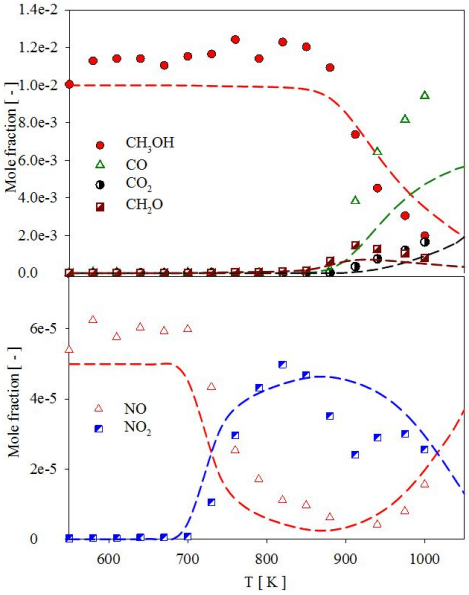

Figure 1: CH_3OH 1 %/O_2 1.5 %/N_2 oxidation in JSR doped with 50 ppm of NO at ϕ = 1.0, P = 1 atm, τ = 0.2 s. Symbols: experimental data from [11], Lines: model prediction.

In addition, NO_2 also reacts with HO_2 to form HNO_2, which isomerizes to form HONO. The formed HONO from the above process thermally decomposes to NO and OH *via* route $NO+OH(+M) \leftrightharpoons HONO(+M)$ which recycles back NO. The other reaction that converts NO to NO_2 is $NO_2+H \leftrightharpoons NO+OH$. It is interesting to observe that as temperature increases above 880 K the NO concentration starts increasing again in the expense of NO_2. This is mainly due to more species at higher temperature participarting in converting NO_2 to HONO which eventually routes back NO *via* $NO+OH(+M) \leftrightharpoons HONO(+M)$. At 1000 K the additional species react with NO_2 to form HONO, which are HCO, CH_2O, CH_3O, and HNO. The formation of more HONO will eventually increase the NO concentration.

Further, CH_3OH oxidation in PFR doped with 215 ppm of NO is shown in Figure 2 studied by Lyon et al. [12] at 1 atm and different residence time. It can be seen that the model predicts the experimental trend at different residence times. However, the model cannot capture the onset of NO oxidation at different residence time. At a residence time of τ = 0.9 s onset of NO oxidation predicted by the model is moved towards higher temperature by 100 K and at a residence times of 0.1 s, 0.048 s, and 0.024 s onset of NO oxidation predicted by the model is higher by 50 K. respectively. The underlying chemistry for the consumption and formation of NO are the same as described in Figure 1.

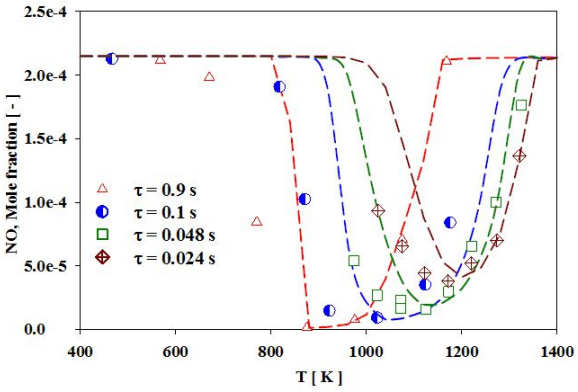

Figure 2: CH_3OH 0.04 %/O_2 5 %/He oxidation in PFR doped with 215 ppm of NO at 1 atm and different residence time. Symbols: experimental measurements from Lyon et al. [12]; lines: model prediction.

Ethanol oxidation in PFR in presence of NO is shown in Figure 3 studied by Alzueta et al. [13]. It can be seen in Figure 3 between 900 – 920 K that the predicted C_2H_5OH conversion is rapid in contrast to the experiments which shows the gradual conversion of C_2H_5OH. It is also worth noting here that at this temperature (900 K) slight reduction of NO and a small peak of NO_2 is observed. C_2H_5OH mainly reacts with OH to form CH_3CHOH (53 %) and CH_2CH_2OH (43 %) as a major product and C_2H_5O (4 %) as a minor product. Conversion of NO to NO_2 is mainly *via* channel $NO+HO_2 \leftrightharpoons NO_2+OH$. As temperature increases above 900 K, further oxidation of C_2H_5OH is promoted by H and O radicals in addition to OH. At 1000 K, C_2H_5OH is also oxidized to form small amount C_2H_4 *via* route $C_2H_5OH(+M) \leftrightharpoons C_2H_4+H_2O$. Further, in Figure 3 it can be observed that until 1100 K we do not have any reasonable decrease in NO nor the NO_2 formation. This is due to the fact the formed NO_2 *via* reaction $NO+HO_2 \leftrightharpoons NO_2+OH$ at this temperature range is rapidly converted back to NO *via* channel $NO_2+H \leftrightharpoons NO+OH$ and $CH_3+NO_2 \leftrightharpoons CH_3O+NO$.

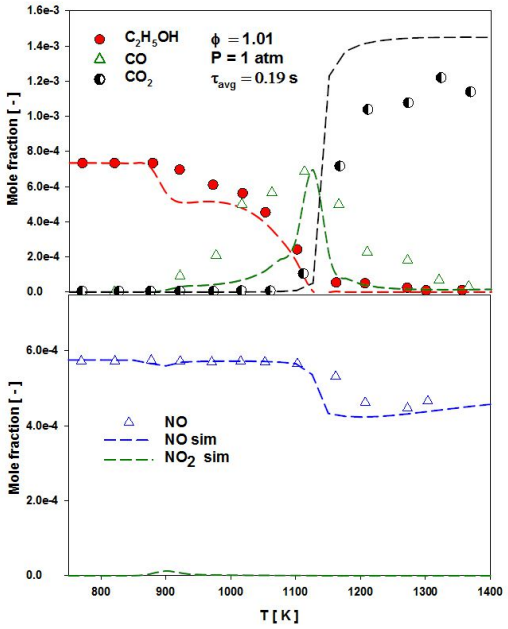

Figure 3: C_2H_5OH 0.0735 %/O_2 0.218 %/H_2O 0.64 %/N_2 oxidation in PFR doped with 576 ppm of NO at ϕ = 1.01, P = 1 atm, τ_{avg} = 0.19 s. Symbols: experimental data from [13], Lines: model prediction.

As temperature increases to 1100 K, NO starts to get consumed as seen in Figure 3. Figure 4 shows the reaction path analysis for NO consumption and formation at 1200 K for the condition shown in Figure 3. At this temperature (1200 K) NO is mainly consumed by reacting with HCCO to form HCNO and HCN *via* reaction HCCO+NO⇋HCNO+CO and HCCO+NO⇋HCN+CO_2 respectively. NO is also converted to N_2O, HONO, and N_2 via other side reactions. NO is converted to N_2O *via* route NH+NO⇋N_2O+H and NCO+NO⇋N_2O+CO. Further, NO is converted to HONO via recombination reaction NO+OH(+M)⇋HONO(+M) and to N_2 *via* reaction N+NO⇋N_2+O. The formed HCNO further reacts with H to form mainly HCN and OH *via* reaction (HCNO+H⇋HCN+OH). The formed HCN in the above process reacts with O to form NCO+H (HCN+O⇋NCO+H).

Further, NCO reacts with NO to give N_2O and N_2 *via* route NCO+NO⇋N_2O+CO and NCO+NO⇋N_2+CO_2 respectively. NCO also reacts with H atom to form NH and CO (NCO+H⇋NH+CO), where NH further reacts with NO to give N_2O and H *via* route NH+NO⇋N_2O+H (not shown in Figure 4). Finally, all the N_2O produced from the above process is completely converted to N_2 *via* reaction N_2O+H⇋N_2+OH. HONO formed *via* recombination of NO and OH reacts with H atom to form HNO and OH (HONO+H⇋HNO+OH).

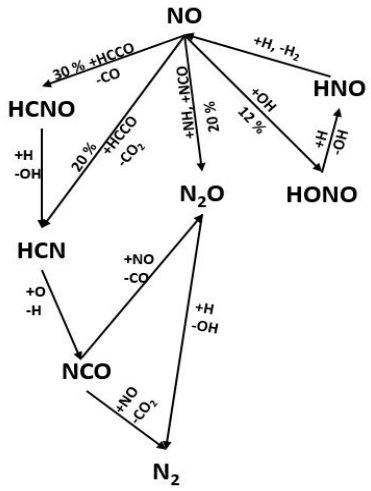

Figure 4: Reaction path analysis for based on nitrogen atom for NO consumption and formation pathways during C_2H_5OH oxidation in PFR shown in Figure 2 at 1200 K.

The formed HNO further reacts with H atom (HNO+H⇋NO+H_2) and thermally decomposes (NO+H(+M) ⇋HNO), which partially recycles the NO. Due to this recycle process, we can see (in Figure 3) a gradual upward trend in NO formation at higher temperatures above 1200 K.

Figure 5 shows the NO formation vs height above the burner (HAB) in premixed burner stabilized flames of methanol/air (a) and ethanol/air (b) at ϕ = 1.15, P = 1 atm and T = 373 K studied by Bohon et al. [14]. In Figure 5 dashed lines represent the model prediction imposing the experimental temperature profile from Bohon et al. [15] and solid lines represent the model prediction solving the energy conservation equation. It can be observed in Figure 5 (a) for CH_3OH/air flame that the model underpredicts the NO concentration imposing the experimental temperature profile as well as using the predicted temperature profile at HAB > 1.5 mm. In C_2H_5OH/air flame shown in Figure 5 (b) model prediction for NO imposing the experimental temperature profile is in good agreement with the measurements while the model underpredicts the NO concentration at HAB > 0.8 mm when using the predicted temperature profile. It is interesting to observe in Figure 5 (a) that for CH_3OH/air flame when solving the energy conservation equation model prediction is higher compared to one predicted imposing the experimental temperature profile. This observation is in contrast to the C_2H_5OH/air flame (Figure 5 (b)) where model prediction solving the energy conservation equation is lower compared to one predicted imposing the experimental temperature profile.

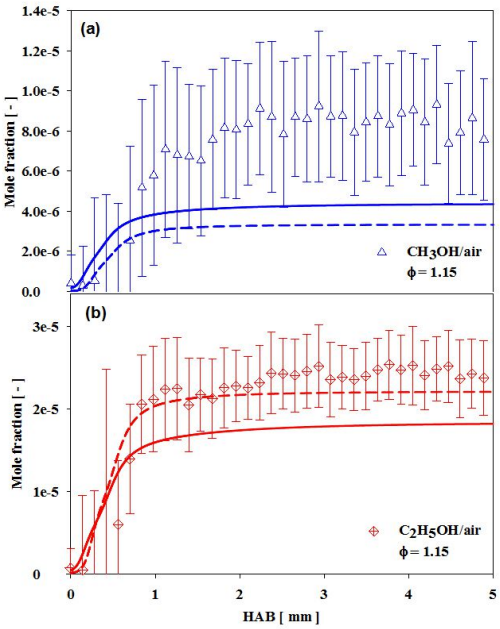

Figure 5: Comparison between the model predicted NO concentration against the measurements in methanol/air (a) and ethanol/air (b) premixed burner-stabilized flame at ϕ = 1.15, 1 atm and 373 K. Symbols: measurements from Bohon et al. [14]; lines: model prediction (dash lines: imposing experimental temperature profile from Bohon et al. [15], solid lines: solving energy conservation equation).

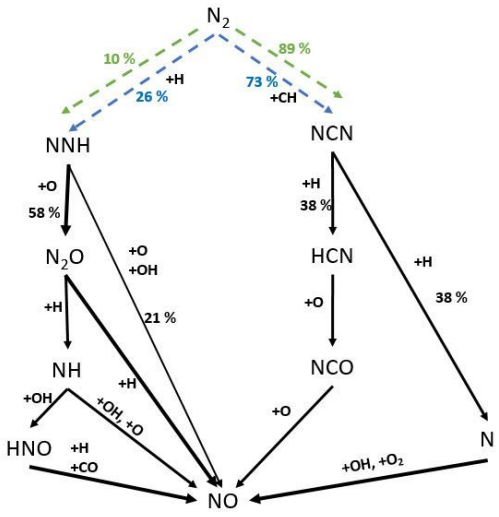

Figure 6: Reaction path analysis based on the integrated nitrogen atom flux at ϕ = 1.15 for the burner stabilized laminar premixed methanol/air (a) and ethanol/air (b) flames shown in Figure 5. Only the initial N_2 consumption step is different, dash blue lines: methanol flame; dash green lines: ethanol flame. The proportion of other channel forming and consuming intermediate products remain the same in both flames and is shown by solid black lines.

Figure 6 shows a reaction path analysis for the major species based on the integrated nitrogen atom flow for laminar premixed burner stabilized methanol/air and ethanol/air flames (Figure 5) at ϕ = 1.15, using the experimental temperature profile. In Figure 6 dashed blue lines for methanol flame and dashed green lines for ethanol flame differentiate only in the initial N_2 consumption. The proportion of consumption and formation of intermediate products *via* the subsequent channel in both the flames remain the same (shown by the solid black lines). We observe that N_2 reacts mainly with H atoms and CH radicals forming NNH and NCN radicals *via* reactions NNH⇋N_2+H and CH+N_2⇋NCN+H respectively. In both the flames, the NCN route is favored compared to the NNH route. In the methanol flame, the NCN path is almost 3 times stronger than the NNH path. In the ethanol flame, this path (NCN) is almost 9 times stronger than the NNH path. However, in the methanol flame, the NNH path is stronger than in the ethanol flame by almost factor 2.5 and the NCN pathway in the ethanol flame is stronger than in the methanol flame by factor 1.2. Other minor channels are responsible for consuming the rest of N_2 in the initial step (not shown in Figure 6).

NNH decomposes producing mainly N_2O and NO *via* reactions NNH+O⇋N_2O+H and NNH+O⇋NO+NH respectively, with the major product being N_2O, which consumes around 58 % of NNH. The proportion of NNH consumption and the reaction channels remain the same in both flames. The formed N_2O reacts with H atoms forming NH and NO *via* reaction channel NH+NO⇋N_2O+H. The formed NH radical reacts with O and OH radicals which mainly forms NO *via* the reaction paths NH+O⇋NO+H and NH+OH⇋NO+H_2, while NH also reacts with OH radical to form HNO and H *via* route NH+OH⇋HNO+H. The formed HNO now further reacts mainly with H and CO, which contributes to the formation of NO *via* the reactions channels HNO+H⇋NO+H_2 and HCO+NO⇋HNO+CO. The cyanonitrene radical (NCN) formed initially through CH+N_2⇋NCN+H reacts mainly with H atoms to form hydrogen cyanide (HCN) and N atoms. The other minor channel, which produces CN and NO consuming NCN (not shown in Figure 6), is *via* the reaction NCN+O⇋CN+NO. The formed HCN from the above process reacts with O radical to form NCO and H; NCO further reacts with O radical to give NO and CO. The minor route that consumes the NCO forms NH (not shown in Figure 6) *via* the reaction NCO+H⇋NH+CO; the NH radical formed here contributes to the NO formation by reacting with OH and O radicals. The N atoms formed *via* the NCN path (NCN+H⇋N+HCN) reacts with O_2 and OH thus contributing to the overall formation of NO *via* route N+O_2⇋NO+O and N+OH⇋NO+H.

Conclusion

A detailed kinetic scheme for the oxidation of methanol and ethanol has been developed successfully extending our previous work. The developed kinetic model also takes into account the reaction pathways for the formation and reduction of NO_x. A number of published experiments has been selected to validate and demonstrate the important features of the CH_3OH and C_2H_5OH chemistry and its cross-reaction with nitrogen chemistry. The model is not able to correctly predict the NO formation in methanol/air premixed flame and this task will be addressed in our future work. In both methanol/air and ethanol/air burner stabilized flames, prompt NO formation is favored *via* the NCN route ($CH+N_2 \leftrightharpoons NCN+H$).

References

[1] K.P. Shrestha, L. Seidel, T. Zeuch, F. Mauss, Energ. Fuels. 32 (2018) 10202−10217.

[2] M.A. Costagliola, L. De Simio, S. Iannaccone, M. V. Prati, Appl. Energy 111 (2013) 1162–1171.

[3] M.B. Çelik, B. Özdalyan, F. Alkan, Fuel. 90 (2011) 1591–1598.

[4] V.R. Surisetty, A.K. Dalai, J. Kozinski, Appl. Catal. A Gen. 404 (2011) 1–11.

[5] A. Neimark, V. Kholmer, E. Sher, in:, SAE Tech. Pap. 940311, 1994.

[6] M.K. Balki, C. Sayin, M. Canakci, Fuel. 115 (2014) 901–906.

[7] M. Eyidogan, A.N. Ozsezen, M. Canakci, A. Turkcan, Fuel. 89 (2010) 2713–2720.

[8] P. Dagaut, O. Mathieu, A. Nicolle, G. Dayma, Combust. Sci. Technol. 177 (2005) 1767–1791.

[9] P. Dagaut, A. Nicolle, Combust. Flame. 140 (2005) 161–171.

[10] D.L. Baulch, C.T. Bowman, C.J. Cobos, R.A. Cox, T. Just, J.A. Kerr, M.J. Pilling, D. Stocker, J. Troe, R.W. Walker, J. Warnatz, D.L. Baulch, J. Phys. Chem. Ref. Data 34 34 (2005) 757–1397.

[11] G. Moréac, Experimental Study and Modelling of Chemical Interactions between Gases Residual and Fresh Gas in the Homogeneous Spontaneous Ignition Gasoline Engines, PhD Thesis, University of Orléans, 2003.

[12] R.K. Lyon, J.A. Cole, J.C. Kramlich, S.L. Chen, Combust. Flame. 81 (1990) 30–39.

[13] M.U. Alzueta, J.M. Hernández, Energ. Fuels. 16 (2002) 166–171.

[14] M.D. Bohon, T.F. Guiberti, W.L. Roberts, Combust. Flame. 194 (2018) 363–375.

[15] M.D. Bohon, T.F. Guiberti, S. Mani Sarathy, W.L. Roberts, Proc. Combust. Inst. 36 (2017) 3995–4002.